The Structure Optimization of Phenanthroimidazole Based Isomers with External Quantum Efficiency Approaching 7% in non-doped Deep-blue OLEDs

Jie-Ji Zhu,[a] Yuwen Chen,[b] Yong-Hong Xiao,[a] Xin Lian,[a] Guo-Xi Yang,[a] Shan-Shun Tang,[a] Dongge Ma,*[b] Ying Wang,[c] and Qing-Xiao Tong*[a]

[a] *Department of Chemistry and Key Laboratory for Preparation and Application of Ordered Structural Material of Guangdong Province, Shantou University, Guangdong, 515063, P. R. China. E-mail: qxtong@stu.edu.cn*

[b] *Institute of Polymer Optoelectronic Materials and Devices, State Key Laboratory of Luminescent Materials and Devices, South China University of Technology, Guangzhou, 510640, People's Republic of China. E-mail: msdgma@scut.edu.cn*

[c] *Key Laboratory of Photochemical Conversion and Optoelectronic Materials, Technical Institute of Physics and Chemistry, Chinese Academy of Sciences, Beijing 100190, China. E-mail: wangy@mail.ipc.ac.cn*

Contants

SI-1. Quantum Chemical Calculations

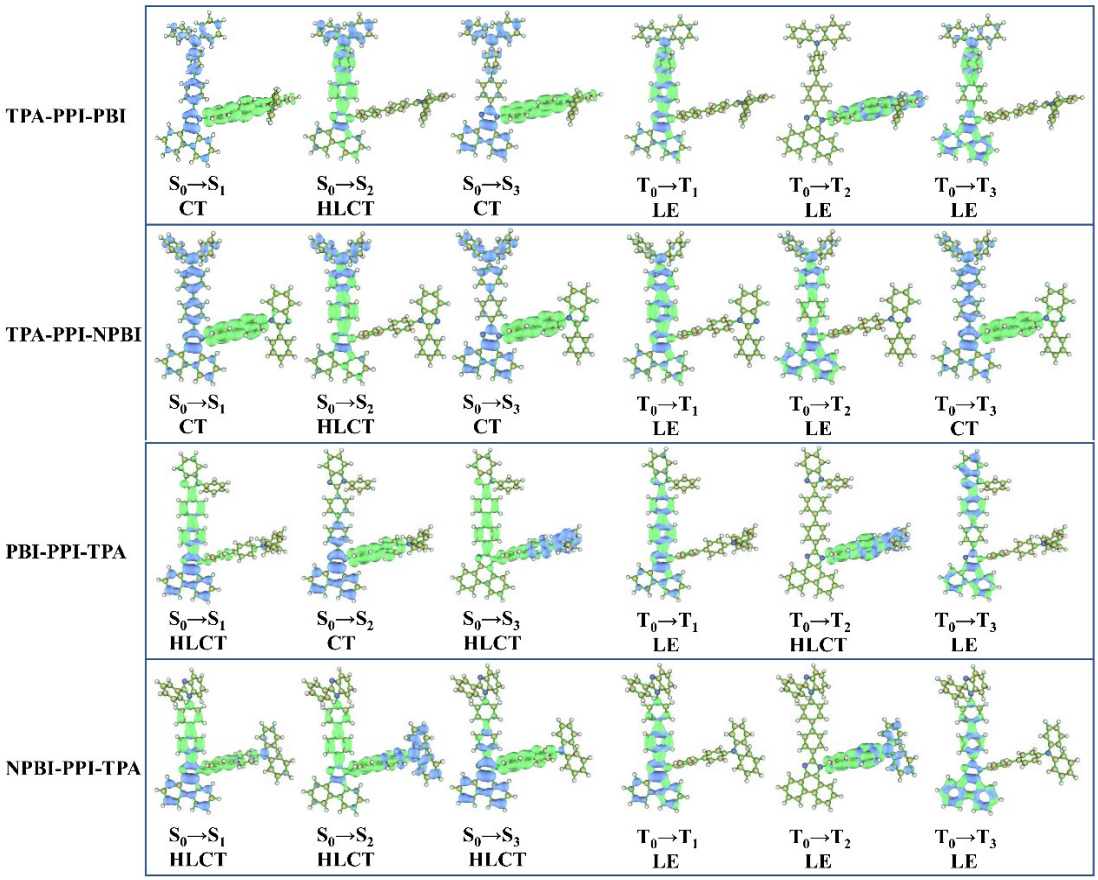

Fig. S1. Natural transition orbitals of $S_0 \rightarrow S_n$ and $T_0 \rightarrow T_n$ (n = 1-3) of four compounds. The blue and green isosurfaces present hole and electron distribution, respectively.

Table S1. The calculated first-ten singlet and triplet states of **TPA-PPI-PBI**.

State	Energy level (eV)	λ_{ex} (nm)	Oscillator strength	State	Energy level (eV)	λ_{ex} (nm)
S_1	2.94	421.7	0.0298	T_1	2.54	488.7
S_2	3.24	383.4	1.2087	T_2	2.77	447.7
S_3	3.27	379.4	0.007	T_3	2.83	439.0
S_4	3.64	340.4	0.0803	T_4	2.95	420.1
S_5	3.69	336.0	0.0533	T_5	3.15	394.3
S_6	3.77	329.0	1.0169	T_6	3.18	390.1
S_7	3.82	325.0	0.0507	T_7	3.26	380.8
S_8	3.85	322.6	0.0596	T_8	3.29	376.7
S_9	3.86	321.6	0.0815	T_9	3.33	372.4
S_{10}	3.90	317.9	0.0199	T_{10}	3.47	357.5

Table S2. The calculated first-ten singlet and triplet states of **TPA-PPI-NPBI**.

State	Energy level (eV)	λ_{ex} (nm)	Oscillator strength	State	Energy level (eV)	λ_{ex} (nm)
S_1	3.02	411.3	0.0662	T_1	2.54	488.8
S_2	3.23	383.8	1.1162	T_2	2.82	439.4
S_3	3.34	371.9	0.0132	T_3	3.02	411.4
S_4	3.62	342.8	0.0231	T_4	3.02	410.6
S_5	3.64	341.1	0.0192	T_5	3.14	395.0
S_6	3.66	339.1	0.0812	T_6	3.15	393.4
S_7	3.78	327.8	0.0434	T_7	3.18	389.6
S_8	3.79	327.2	0.0197	T_8	3.31	374.6
S_9	3.85	322.2	0.0121	T_9	3.36	369.7
S_{10}	3.89	318.9	0.0295	T_{10}	3.47	357.1

Table S3. The calculated first-ten singlet and triplet states of **PBI-PPI-TPA**.

State	Energy level (eV)	λ_{ex} (nm)	Oscillator strength	State	Energy level (eV)	λ_{ex} (nm)
S_1	3.25	382.3	1.0073	T_1	2.54	488.2
S_2	3.39	366.0	0.162	T_2	2.74	452.1
S_3	3.42	362.8	0.3285	T_3	2.83	438.1
S_4	3.51	353.8	0.4735	T_4	3.08	403.5
S_5	3.59	345.5	0.0015	T_5	3.21	386.2
S_6	3.69	335.8	0.5018	T_6	3.32	373.9
S_7	3.75	331.2	0.0116	T_7	3.36	368.8
S_8	3.82	324.7	0.0028	T_8	3.40	364.6
S_9	3.87	320.6	0.0019	T_9	3.44	360.2
S_{10}	3.92	316.4	0.0344	T_{10}	3.49	355.5

Table S4. The calculated first-ten singlet and triplet states of **NPBI-PPI-TPA**.

State	Energy level (eV)	λ_{ex} (nm)	Oscillator strength	State	Energy level (eV)	λ_{ex} (nm)
S_1	3.34	371.9	0.6616	T_1	2.59	478.9
S_2	3.42	363.1	0.4296	T_2	2.75	451.7
S_3	3.45	359.3	0.2827	T_3	2.97	418.3
S_4	3.49	355.2	0.2837	T_4	3.02	410.7
S_5	3.78	328.7	0.0058	T_5	3.21	386.0
S_6	3.81	325.7	0.0153	T_6	3.34	372.0
S_7	3.87	320.8	0.0106	T_7	3.35	370.5
S_8	3.94	315.0	0.0474	T_8	3.44	360.9
S_9	3.96	313.0	0.0244	T_9	3.44	360.4
S_{10}	4.00	310.2	0.0993	T_{10}	3.49	355.4

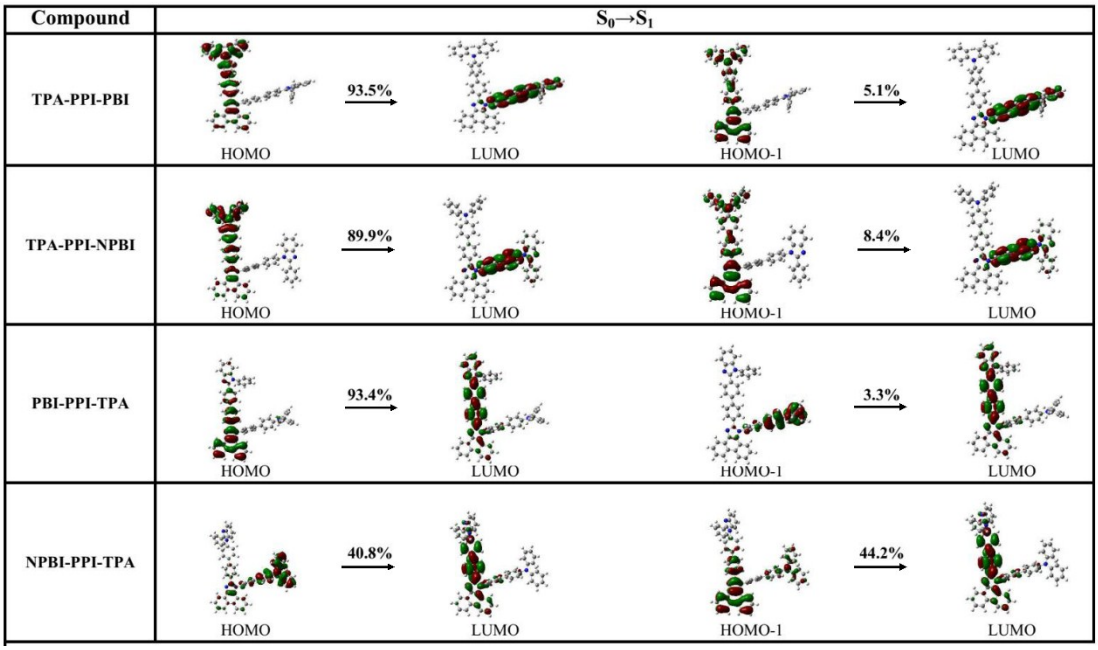

Fig. S2. The major molecular orbital contribution to $S_0 \rightarrow S_n$ transfer of new compounds.

SI-2. Photophysical properties

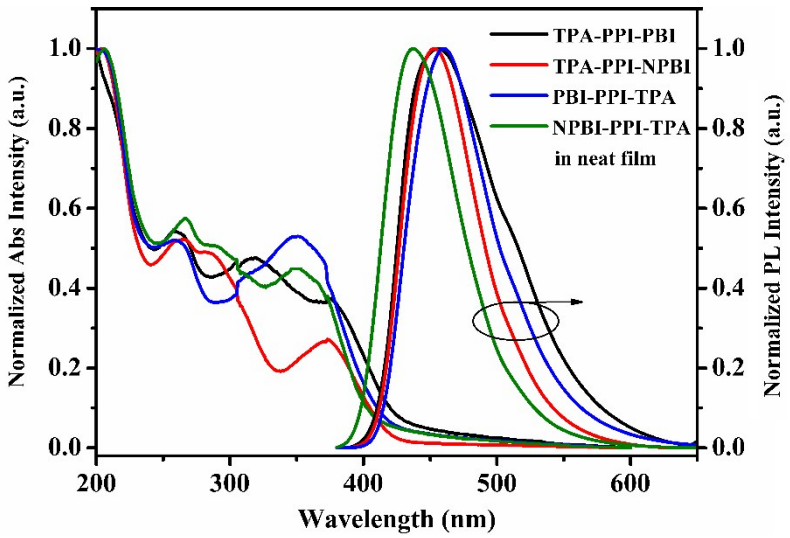

Fig. S3. Normalized UV/Vis absorption and PL spectra of new compounds in neat film.

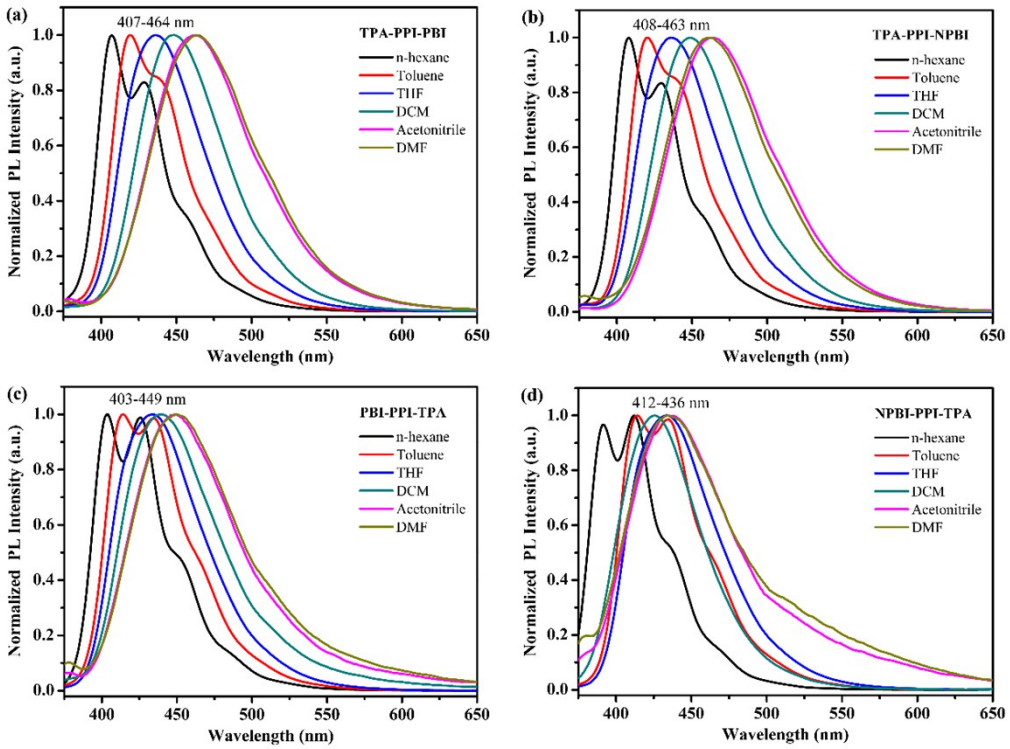

Fig. S4. Normalized fluorescence spectra of new compounds in different solvents.

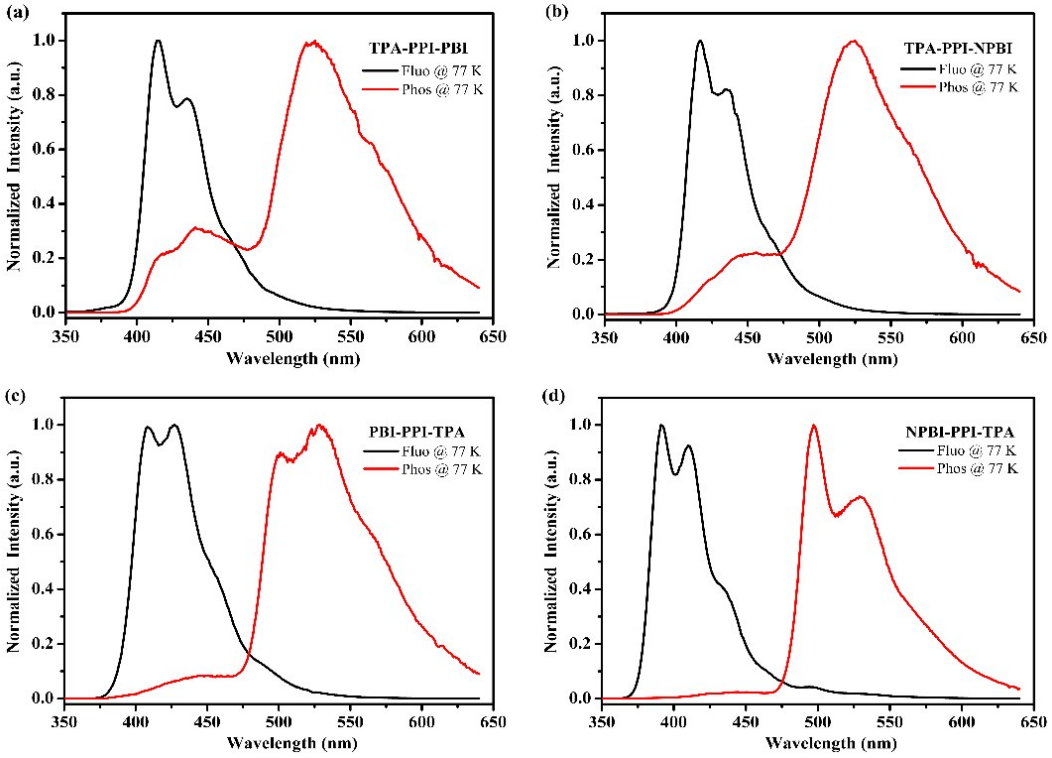

Fig. **S5**. Normalized fluorescence and phosphorene spectra of new compounds at 77 K.

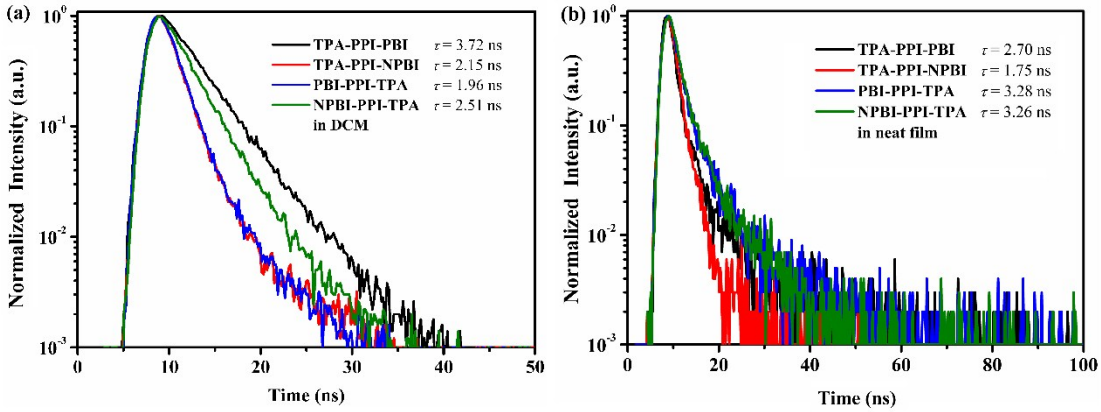

Fig. S6. Lifetime measurement of new compounds in degassed DCM (a) and neat film (b).

SI-3. Crystal structure

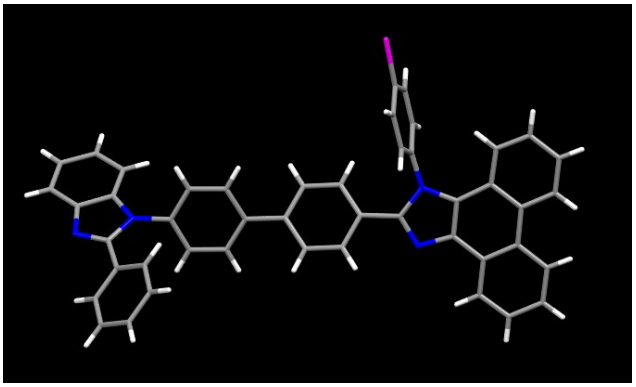

Fig. S7. Crystal structure of intermediate **NPBI-PPI-Br**.

SI-4. Distributions of the molecular frontier orbitals

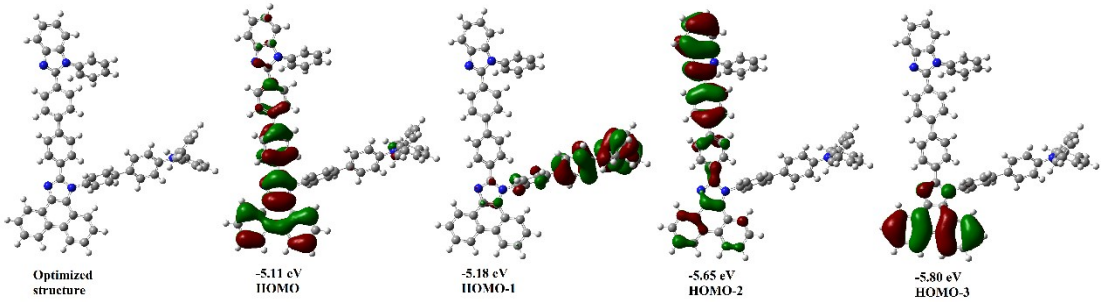

Fig. S8. The HOMOs distribution and energy levels of **PBI-PPI-TPA**.

SI-5. Electroluminescence spectra

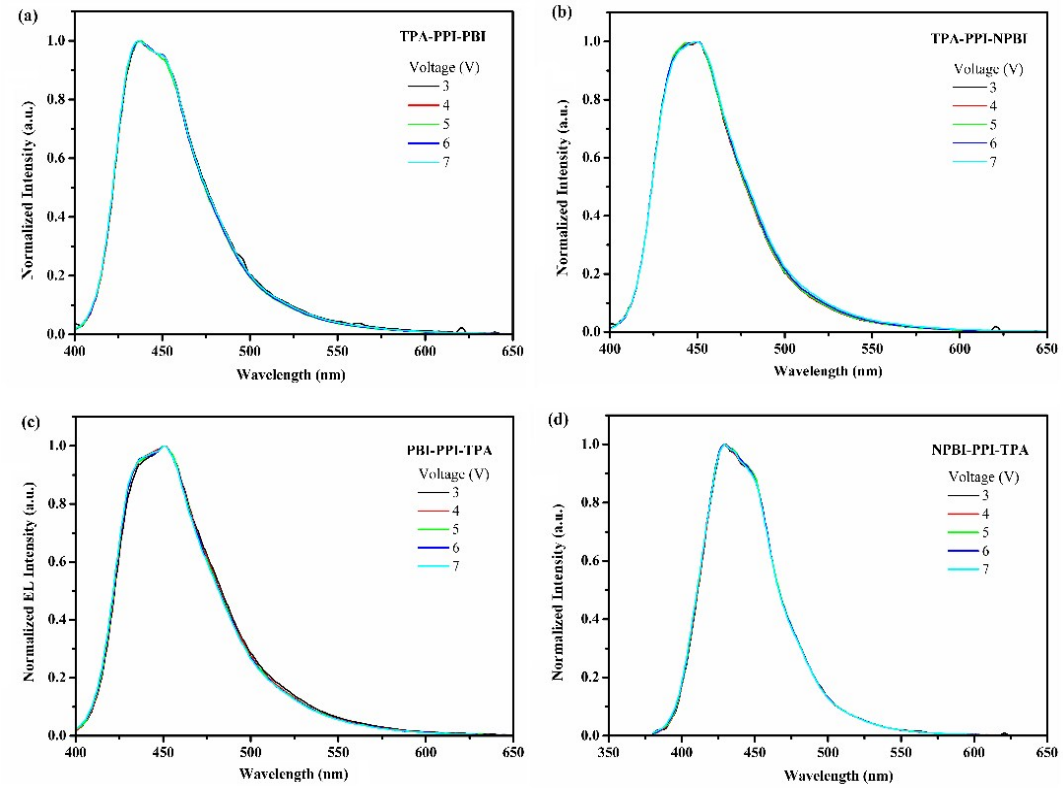

Fig. S9. Electroluminescence spectra of new compounds at different voltage

SI-6. Current density versus voltage characteristics

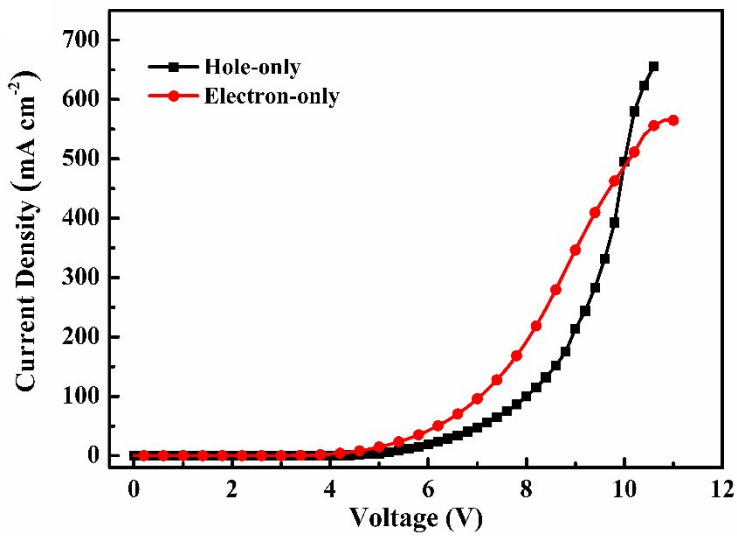

Fig. S10. Current density versus voltage characteristics of hole-only device and electron-only device of **PBI-PPI-TPA**.

SI-7. NMR spectra

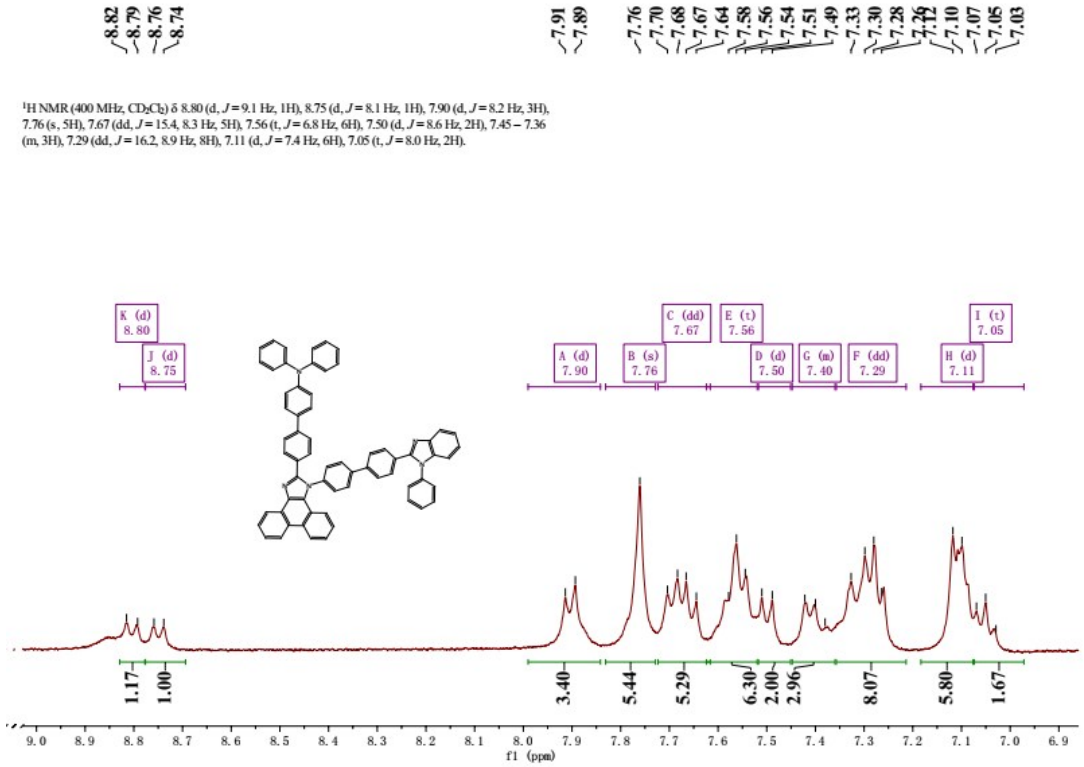

^{1}H NMR (400 MHz, CD_2Cl_2) δ 8.80 (d, *J* = 9.1 Hz, 1H), 8.75 (d, *J* = 8.1 Hz, 1H), 7.90 (d, *J* = 8.2 Hz, 3H), 7.76 (s, 5H), 7.67 (dd, *J* = 15.4, 8.3 Hz, 5H), 7.56 (t, *J* = 6.8 Hz, 6H), 7.50 (d, *J* = 8.6 Hz, 2H), 7.45 – 7.36 (m, 3H), 7.29 (dd, *J* = 16.2, 8.9 Hz, 8H), 7.11 (d, *J* = 7.4 Hz, 6H), 7.05 (t, *J* = 8.0 Hz, 2H).

Fig. S11 ^{1}H NMR spectrum of **TPA-PPI-PBI** in CD_2Cl_2.

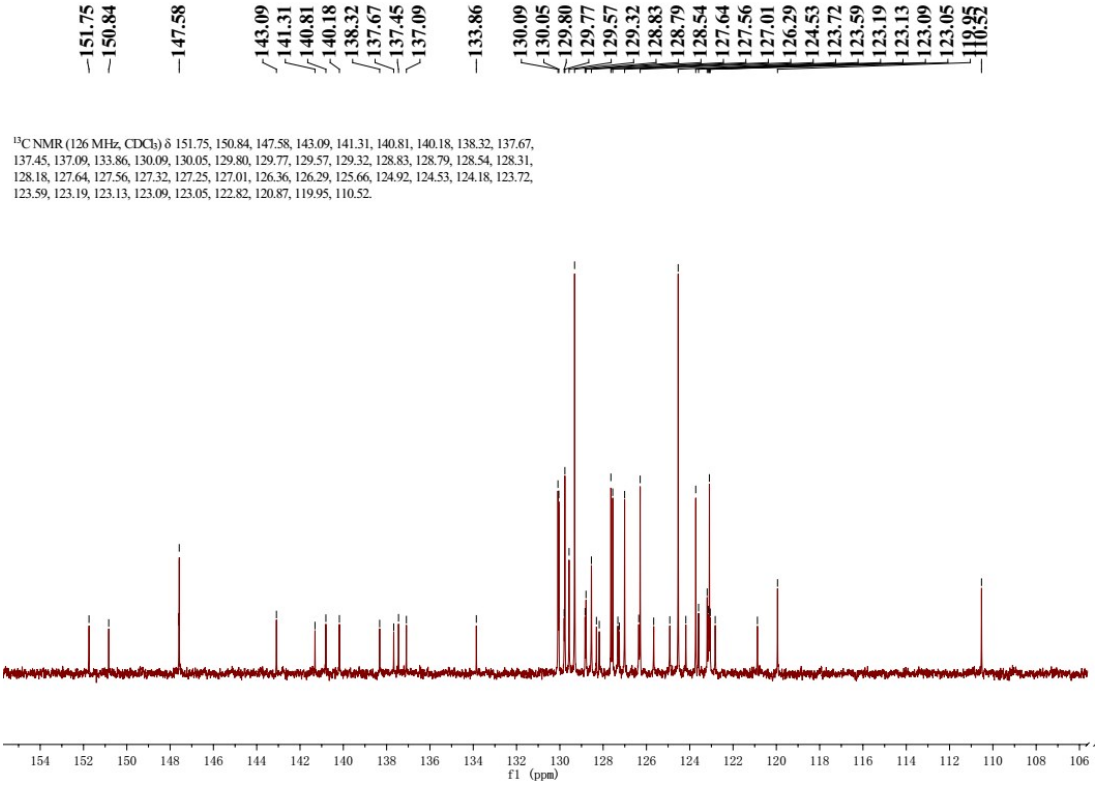

^{13}C NMR (126 MHz, $CDCl_3$) δ 151.75, 150.84, 147.58, 143.09, 141.31, 140.81, 140.18, 138.32, 137.67, 137.45, 137.09, 133.86, 130.09, 130.05, 129.80, 129.77, 129.57, 129.32, 128.83, 128.79, 128.54, 128.31, 128.18, 127.64, 127.56, 127.32, 127.25, 127.01, 126.36, 126.29, 125.66, 124.92, 124.53, 124.18, 123.72, 123.59, 123.19, 123.13, 123.09, 123.05, 122.82, 120.87, 119.95, 110.52.

Fig. S12 ^{13}C NMR spectrum of **TPA-PPI-PBI** in $CDCl_3$.

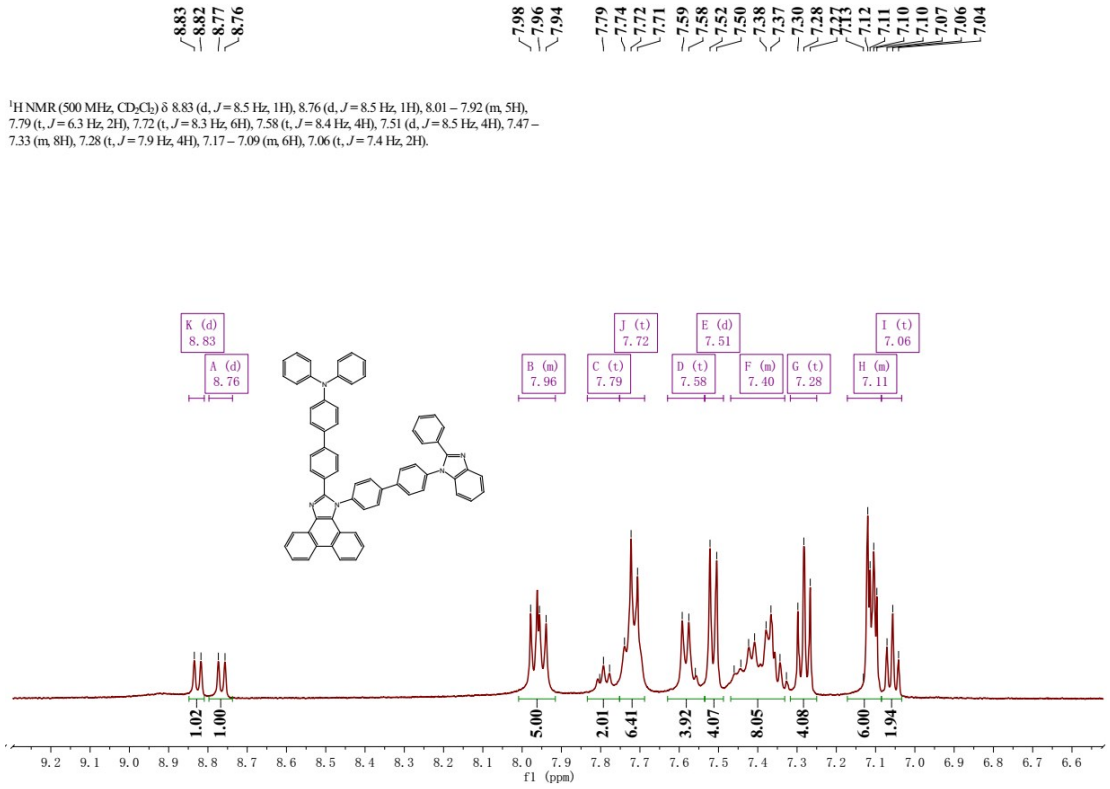

^{1}H NMR (500 MHz, CD_2Cl_2) δ 8.83 (d, *J* = 8.5 Hz, 1H), 8.76 (d, *J* = 8.5 Hz, 1H), 8.01 – 7.92 (m, 5H), 7.79 (t, *J* = 6.3 Hz, 2H), 7.72 (t, *J* = 8.3 Hz, 6H), 7.58 (t, *J* = 8.4 Hz, 4H), 7.51 (d, *J* = 8.5 Hz, 4H), 7.47 – 7.33 (m, 8H), 7.28 (t, *J* = 7.9 Hz, 4H), 7.17 – 7.09 (m, 6H), 7.06 (t, *J* = 7.4 Hz, 2H).

Fig. S13 ^{1}H NMR spectrum of **TPA-PPI-NPBI** in CD_2Cl_2.

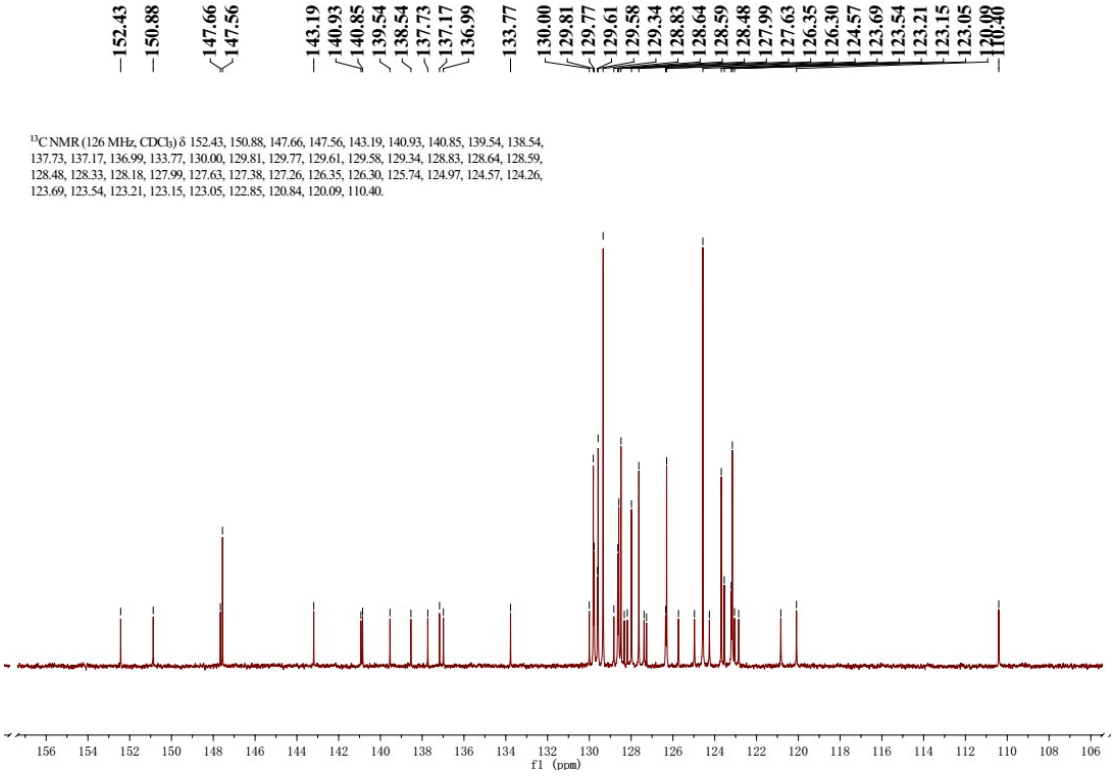

^{13}C NMR (126 MHz, $CDCl_3$) δ 152.43, 150.88, 147.66, 147.56, 143.19, 140.93, 140.85, 139.54, 138.54, 137.73, 137.17, 136.99, 133.77, 130.00, 129.81, 129.77, 129.61, 129.58, 129.34, 128.83, 128.64, 128.59, 128.48, 128.33, 128.18, 127.99, 127.63, 127.38, 127.26, 126.35, 126.30, 125.74, 124.97, 124.57, 124.26, 123.69, 123.54, 123.21, 123.15, 123.05, 122.85, 120.84, 120.09, 110.40.

Fig. S14 ^{13}C NMR spectrum of **TPA-PPI-NPBI** in $CDCl_3$.

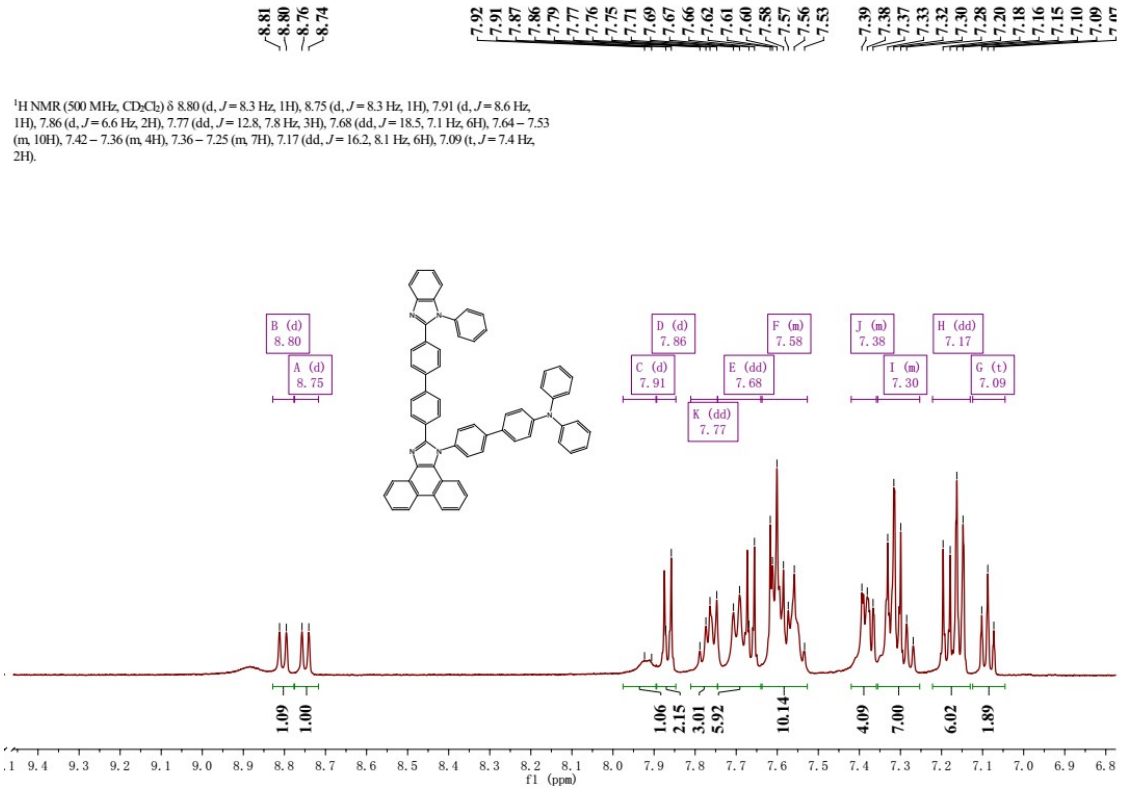

Fig. S15 ^{1}H NMR spectrum of **PBI-PPI-TPA** in CD_2Cl_2.

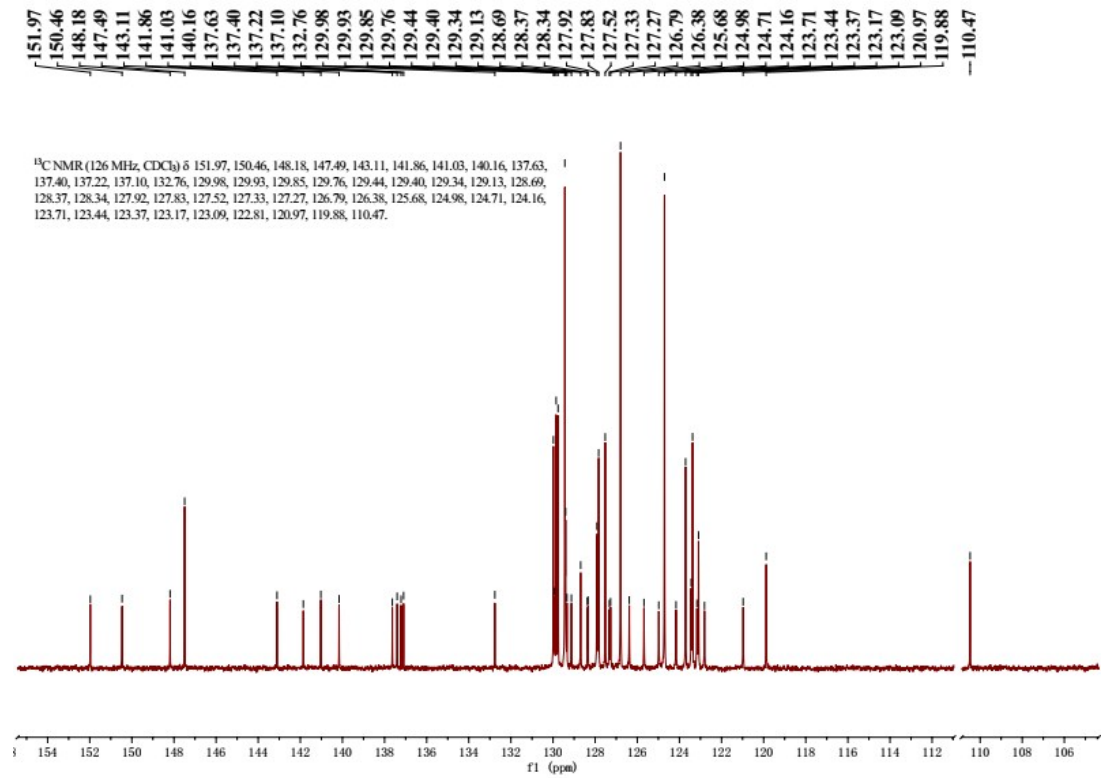

Fig. S16 ^{13}C NMR spectrum of **PBI-PPI-TPA** in $CDCl_3$.

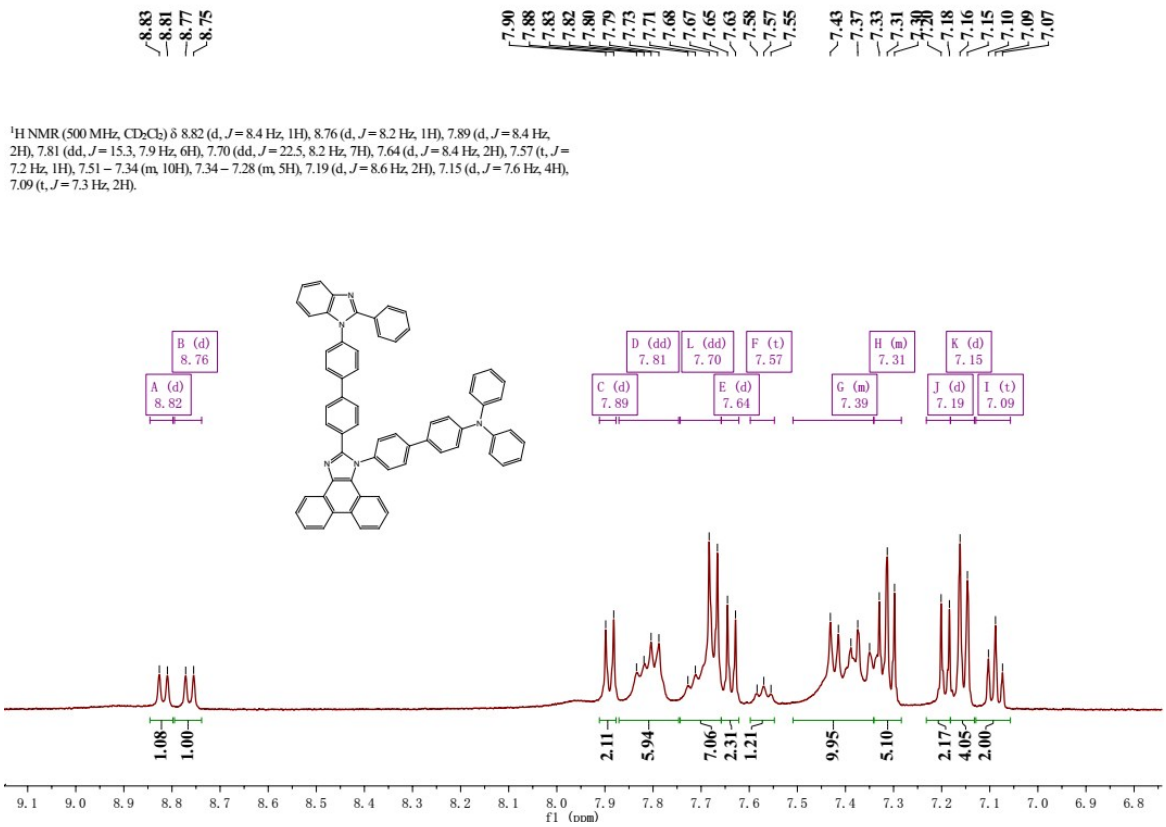

^{1}H NMR (500 MHz, CD_2Cl_2) δ 8.82 (d, *J* = 8.4 Hz, 1H), 8.76 (d, *J* = 8.2 Hz, 1H), 7.89 (d, *J* = 8.4 Hz, 2H), 7.81 (dd, *J* = 15.3, 7.9 Hz, 6H), 7.70 (dd, *J* = 22.5, 8.2 Hz, 7H), 7.64 (d, *J* = 8.4 Hz, 2H), 7.57 (t, *J* = 7.2 Hz, 1H), 7.51 – 7.34 (m, 10H), 7.34 – 7.28 (m, 5H), 7.19 (d, *J* = 8.6 Hz, 2H), 7.15 (d, *J* = 7.6 Hz, 4H), 7.09 (t, *J* = 7.3 Hz, 2H).

Figure S17 ^{1}H NMR spectra of **NPBI-PPI-TPA** in CD_2Cl_2.

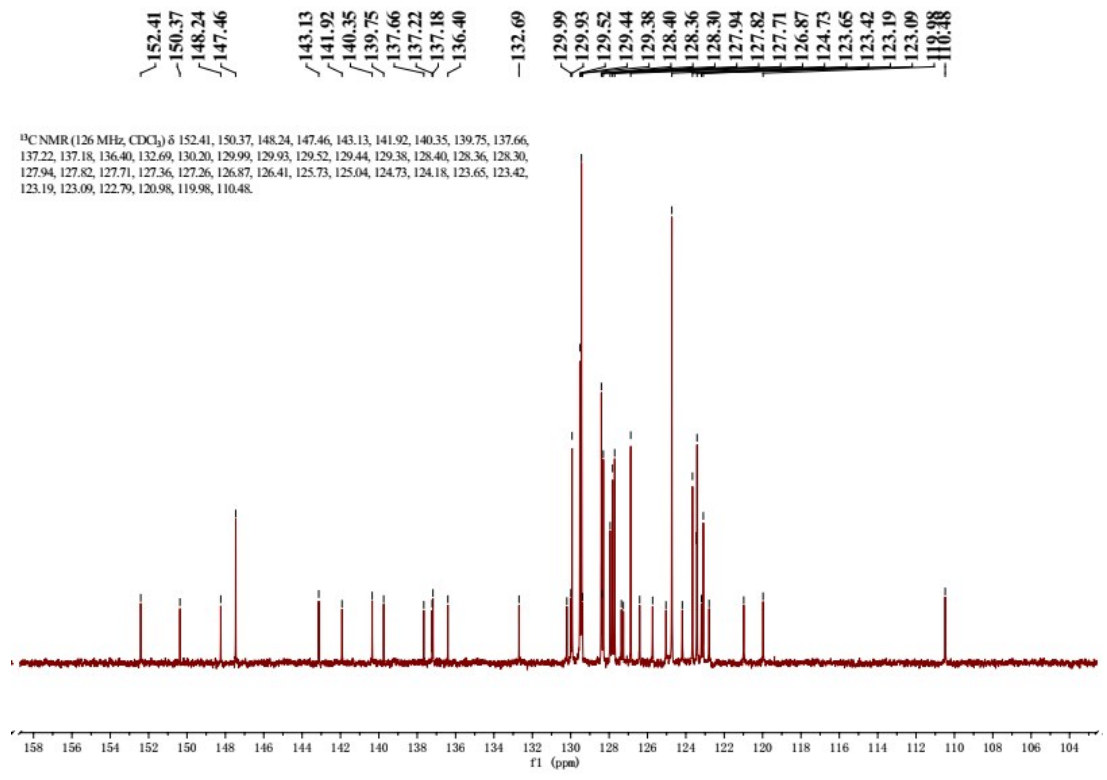

^{13}C NMR (126 MHz, $CDCl_3$) δ 152.41, 150.37, 148.24, 147.46, 143.13, 141.92, 140.35, 139.75, 137.66, 137.22, 137.18, 136.40, 132.69, 130.20, 129.99, 129.93, 129.52, 129.44, 129.38, 128.40, 128.36, 128.30, 127.94, 127.82, 127.71, 127.36, 127.26, 126.87, 126.41, 125.73, 125.04, 124.73, 124.18, 123.65, 123.42, 123.19, 123.09, 122.79, 120.98, 119.98, 110.48.

Figure S18 ^{13}C NMR spectra of **NPBI-PPI-TPA** in $CDCl_3$.